Hartman, M., and R. W. Coughlin, "Reaction of Sulfur Dioxide with Limestone and the Influence of Pore Structure," *Ind. Eng. Chem. Proc. Des. Dev.*, 13, 248 (1974).
Hartman, M., and R. W. Coughlin, "Reaction of Sulfur Dioxide with Limestone and the Grain Model," *AIChE J.*, 22, 490 (1976).
Hauffe, K., "Gas-solid Reactions—Oxidation," in Treatise on Solid State Chemistry, 4, 389, N. B. Hannay, ed., Plenum Press, New York (1976).
McClellan, G. H., and J. L. Eades, "The Textural Evolution of Limestone Calcines," *The Reaction Parameters of Lime*, ASTM Special Tech. Pub. 472, 209 (1970).
Mullins, R. C., and J. D. Hatfield, "Effects of Calcination Conditions on the Properties of Lime," *The Reaction Parameters of Lime*, ASTM Special Tech. Pub. 472, 117 (1970).
Potter, A. E., "Sulfur Oxide Capacity of Limestones," *Am. Ceram. Soc. Bull.*, 48, 855 (1969).
Pigford, R. L., and G. Sliger, "Rate of Diffusion Controlled Reaction between a Gas and a Porous Solid Sphere," *Ind. Eng. Chem. Proc. Des. Dev.*, 12, 85 (1973).
Ramachandran, P. A., and J. M. Smith, "A Single-Pore Model for Gas-Solid Non-Catalytic Reactions," *AIChE J.*, 23, 353 (1977).
Szekely, J., J. W. Evans, and H. Y Sohn, *Gas-Solid Reactions*, Academic Press, London (1976).
Ulerich, N. H., E. P. O'Neill, and D. L. Keairns, "A Thermogravimetric Study of the Effect of Pore Volume—Pore Size Distribution on the Sulfation of Calcined Limestone," *Thermochimica Acta*, 26, 269 (1978).
Wen, C. Y., and M. Ishida, "Reaction of Sulfur Dioxide with Particles Containing Calcium Oxide," *Environ. Sci. Technol.*, 7, 703 (1973).

Manuscript received February 29, 1980; revision received July 14, and accepted July 16, 1980.

Wrong-Way Behavior of Packed-Bed Reactors:

1. The Pseudo-Homogeneous Model

P. S. MEHTA
W. N. SAMS
and
D. LUSS

Department of Chemical Engineering
University of Houston
Houston, Texas 77004

A sudden reduction in the feed temperature to a packed-bed reactor leads to a transient temperature rise, which is referred to as the wrong-way behavior. A pseudo-homogeneous plug-flow model is used to analyze the structure of this transient behavior. The key parameters which determine the magnitude of this response are the dimensionless adiabatic temperature rise, activation energy, heat transfer capacity, coolant temperature, magnitude of temperature drop and length of the reactor. A simple expression is derived for predicing the maximum transient temperature rise.

SCOPE

When the temperature of the feed to a packed-bed reactor is suddenly decreased a transient temperature rise may occur. This surprising dynamic feature is caused by the difference in the speed of propagation of the concentration and temperature disturbances and is referred to as the wrong-way behavior. This response was predicted originally by Boreskov and Slinko (1965) and Crider and Foss (1966), and was observed by many investigators (Hoiberg et al., 1971; Van Doesberg and DeJong, 1976a, 1976b; Hansen and Jorgensen, 1977; Sharma and Hughes, 1979).

The wrong-way behavior may damage the catalyst and initiate undesired side reactions. The need to avoid it complicates the control policies and start-up and shut-down procedures of packed-bed reactors. At present lengthy numerical simulations are required to determine when this behavior may be encountered and its magnitude.

The purpose of this work is to identify the key rate processes and parameters which cause this behavior and to develop a simple technique for a priori prediction of the highest transient temperature without solving the transient equations. This is accomplished by analyzing the dynamic response of a plug-flow pseudo-homogeneous model of a packed-bed reactor using the method of characteristics. First, we determine the structure of the solution and the conditions for which a wrong-way behavior occurs for a zeroth-order reaction in either a cooled or an adiabatic reactor. We examine then how this behavior is modified by a rate expression for which the reactants are not completely consumed and by intraparticle diffusional resistances.

CONCLUSIONS AND SIGNIFICANCE

The analysis indicates that for a zeroth-order reaction the wrong-way behavior occurs only if the reactor is longer than a critical length of z_{ci}. The highest transient temperature increases with reactor length until the reactor is of length z_{cn}. For any reactor shorter than z_{cn} and longer than z_{ci} the highest transient temperature is encountered at the exit of the reactor. For a cooled reactor longer than z_{cn} the limiting transient-peak temperature occurs at z_{cn}. For an adiabatic reactor the limiting transient-peak temperature is encountered at all points downstream of z_{cn}.

0001-1541-81-4378-0234-$2.00.

When a first-order reaction takes place in an adiabatic reactor a transient temperature overshoot occurs in a reactor of any length. However, this transient temperature exceeds the original adiabatic temperature of $1+\beta$ only if the length of the reactor exceeds a critical value. The highest transient temperature occurs always at the exit of the reactor.

The limiting transient-peak temperature for any nth-order reaction in an adiabatic reactor can be determined either by solving the algebraic Eq. 34 or by integration of Eq. 41. It depends only on the dimensionless adiabatic temperature rise, the activation energy and the new feed temperature. For a zeroth-order reaction in a cooled reactor the limiting transient-peak temperature depends also on the dimensionless heat transfer capacity and the coolant temperature. It can be determined by a simultaneous integration of Eqs. 39 and 40. Numerical examples indicate that a sudden temperature decrease may lead to a very high temperature excursion and should be avoided. In certain cases the temperature peak in a cooled reactor may exceed that attained in an adiabatic reactor, in which the same reaction is carried out.

The simple model used here enables a graphical construction of the transient profiles for a zeroth-order reaction. The method uses two steady-state profiles and the line of zero concentration and requires no additional numerical computations. For the adiabatic first-order reaction a method is developed for decoupling the equations describing the transient temperature and concentration. Once the steady-state profiles have been obtained the temperature at any point within the region of influence of the disturbance can be determined by integration of the single ordinary differential Eq. 44. The inclusion of intraparticle concentration gradients decreases the magnitude of the transient temperature rise and increases the time during which excessive temperatures may occur. The predictions of this model provide useful insight into the wrong-way behavior and can serve as a baseline against which predictions of more refined and complex models can be compared.

One of the most interesting dynamic responses of packed-bed reactors is the so called wrong-way behavior which refers to a transient temperature rise in the reactor caused by a rapid decrease in the feed temperature. This phenomenon was predicted first by Boreskov and Slinko (1965), and Crider and Foss (1966). It was observed by Hoiberg et al. (1971) for a homogeneous liquid-phase reaction in a packed-bed, by Van Doesberg and DeJong (1976a, 1976b) in the catalytic methanation of carbon monoxide, and by Hansen and Jorgensen (1974) and Sharma and Hughes (1979) in the oxidation of carbon monoxide. McGreavy and Naim (1977) discovered this behavior during the dynamic simulation of a packed-bed reactor in which several reactions occur. Eigenberger (1974) has shown that a wrong-way behavior may occur even in an empty tubular reactor when the influence of the wall is significant. Sampath et al. (1975) observed a similar response in the simulation of a noncatalytic gas-solid packed-bed reactor.

The wrong-way behavior is caused by the different speeds of propagation of concentration and temperature disturbances in the bed. The cold feed cools the upstream section of the reactor, and decreases the reaction rate and conversion in that region. The cold fluid with higher than usual concentration of unconverted reactant eventually contacts hot catalyst particles in the downstream section of the bed. This leads to a very rapid reaction and a vigorous rate of heat release, which causes a transient temperature rise. The behavior resembles the well known inverse response of lumped-parameter systems, in which an output variable moves initially in the opposite direction of where it eventually ends up (Luyben 1973; Auslander et al., 1974).

The wrong-way behavior may complicate considerably the control and start-up of packed-bed reactors. The transient peak temperature may surpass the highest steady-state temperature and can damage the catalyst or initiate undesired side reactions leading to a runaway. Moreover, when multiple steady states can exist the wrong-way behavior may shift the reactor to an undesired steady state, as observed by Sharma and Hughes (1979) during the oxidation of carbon monoxide.

At present, no information or criteria are available for predicting the conditions under which the wrong-way behavior exists or its magnitude. Hence, lengthy numerical calculations are used to determine its occurrence. The goal of this work is to develop an understanding of the conditions under which this interesting dynamic response appears and to develop simple criteria predicting its magnitude.

MATHEMATICAL MODEL

We study the wrong-way behavior by analyzing the response of a packed-bed reactor, in which a single exothermic reaction occurs, to a sudden decrease in the feed temperature. A plug-flow pseudo-homogeneous model is used in the analysis. This simple model is not capable of describing some important behavioral features of the reactor such as steady-state multiplicity. However, this model enables a rapid determination of the structure of the transient behavior and a clear demarcation of the key parameters. In addition, its analysis gives valuable insight into the conditions under which this phenomenon may occur.

In this paper, we study the dynamic response of an adiabatic or a cooled reactor in which a zeroth-order reaction occurs, and that of an adiabatic reactor in which a first-order reaction occurs. We also develop a procedure for calculating the limiting transient-peak temperature following a rapid decrease in the feed temperature to an adiabatic packed-bed reactor in which an irreversible nth-order reaction is carried out.

The model neglects axial dispersion of both species and energy and assumes that the temperature and concentration are independent of radial position so that the independent variables are to be interpreted as cross-section averages. For simplicity, we assume constant physical properties and neglect the influence of temperature on the velocity. Defining

$$x = C_A/C_{Ao} \qquad y = T/T_o$$

$$y_w = T_w/T_o \qquad \gamma = E/RT_o$$

$$f = \frac{\hat{k}(T)}{\hat{k}(T_o)} = \exp\left[\gamma\left(1-\frac{1}{y}\right)\right] \qquad z = \frac{\hat{k}(T_o)C_{Ao}^{n-1}z'}{u} \tag{1}$$

$$\beta = \frac{(-\Delta H)C_{Ao}}{\rho_f c_f T_o} \qquad U = \frac{2C_{Ao}^{1-n}U'}{R_t\rho_f c_f \hat{k}(T_o)\epsilon}$$

$$t = \frac{\epsilon\hat{k}(T_o)C_{Ao}^{n-1}t'}{\epsilon + (1-\epsilon)\epsilon_p + (1-\epsilon)(1-\epsilon_p)\rho_s c_s/\rho_f c_f}$$

$$v_c = 1 + \frac{(1-\epsilon)(1-\epsilon_p)}{\epsilon + (1-\epsilon)\epsilon_p}\frac{\rho_s c_s}{\rho_f c_f}$$

the dimensionless species and energy balances are:

$$\frac{1}{v_c}\frac{\partial x}{\partial t} + \frac{\partial x}{\partial z} = -x^n H(x) f(y) \tag{2}$$

$$\frac{\partial y}{\partial t} + \frac{\partial y}{\partial z} = \beta x^n H(x) f(y) + U(y_w - y) \tag{3}$$

where $H(x)$ is the Heaviside function. The corresponding boundary and initial conditions are:

$$x(z, o) = x_i(z) \tag{4a}$$

$$y(z, o) = y_i(z) \tag{4b}$$

$$x(o, t) = 1 \tag{4c}$$

$$y(o, t) = \begin{cases} 1 & t < 0 \\ \theta & t \geq 0 \end{cases} \tag{4d}$$

where the steady-state profiles $x_i(z)$ and $y_i(z)$ are the solutions of:

$$\frac{dx_s}{dz} = -x_s^n H(x_s) f(y_s) \tag{5}$$

$$\frac{dy_s}{dz} = \beta x_s^n H(x_s) f(y_s) + U(y_w - y_s). \tag{6}$$

In particular, the profiles x_i and y_i correspond to the boundary conditions $x_s(o) = 1$ and $y_s(o) = 1$. The solutions of Eqs. 5 and 6 with $x_s(o) = 1$ and $y_s(o) = \theta$ are denoted by $x_n(z)$ and $y_n(z)$. The adiabatic case is obtained by setting $U = o$ in Eqs. 3 and 6. It is well known that for nth-order reactions with $n < 1$ the reactants are completely consumed at a finite distance, denoted by z_c. If $n \geq 1$ the reactants are never completely consumed.

We shall examine later the influence of intraparticle concentration gradients in the special case of a first-order reaction. In this case, $f(y)$ in Eqs. 2, 3, 5 and 6 has to be multiplied by the effectiveness factor η which depends on y and the Thiele modulus

$$\phi_o \triangleq \frac{V_p}{S_x} \sqrt{\hat{k}(T_o)/D_e}. \tag{7}$$

Steady-State Analysis

The steady-state temperature in an adiabatic reactor in which an nth-order exothermic reaction occurs increases monotonically in the downstream direction. If $n < 1$ the reactants are consumed at z_c, and the temperature remains constant for all $z > z_c$. In a cooled reactor with a zeroth-order reaction three types of temperature profiles exist in the region in which the reactants are not completely consumed. If the feed temperature is y_o and

$$f(y_o) + U(y_w - y_o)/\beta = 0 \tag{8}$$

then

$$y(z) = y_o \tag{9}$$

for all $z \leq z_c$. If Eq. 8 is not satisfied integration of Eq. 6 gives

$$\beta z = \int_{y_o}^{y} \frac{dy'}{F(y')} \tag{10}$$

where

$$F(y) \triangleq f(y) + U(y_w - y)/\beta. \tag{11}$$

According to Eq. 10, $F(y)$ cannot vanish for any finite z, so that dy/dz cannot change its sign for $z \leq z_c$. Thus, if $F(y_o) > 0$ the temperature increases monotonically for $z \leq z_c$. For all $z > z_c$, the temperature approaches asymptotically y_w and is given by:

$$y(z) - y_w = [y(z_c) - y_w] \exp[-U(z - z_c)] \qquad z > z_c. \tag{12}$$

Thus, when $F(y_o) > 0$ points with the same temperature exist on either side of z_c. This introduces distinctive features which are not found in an adiabatic reactor. The sign of $F(y_o)$ depends on the location of y_o relative to the zeroes of $F(y)$. When $F(y)$ has a unique zero, y_1, then $F(y_o)$ is positive if $y_o < y_1$ and negative otherwise. When $F(y)$ has three zeroes y_1, y_2, and y_3 then $F(y_o)$ is positive if either $y_o < y_1$ or $y_2 < y_o < y_3$, and negative otherwise.

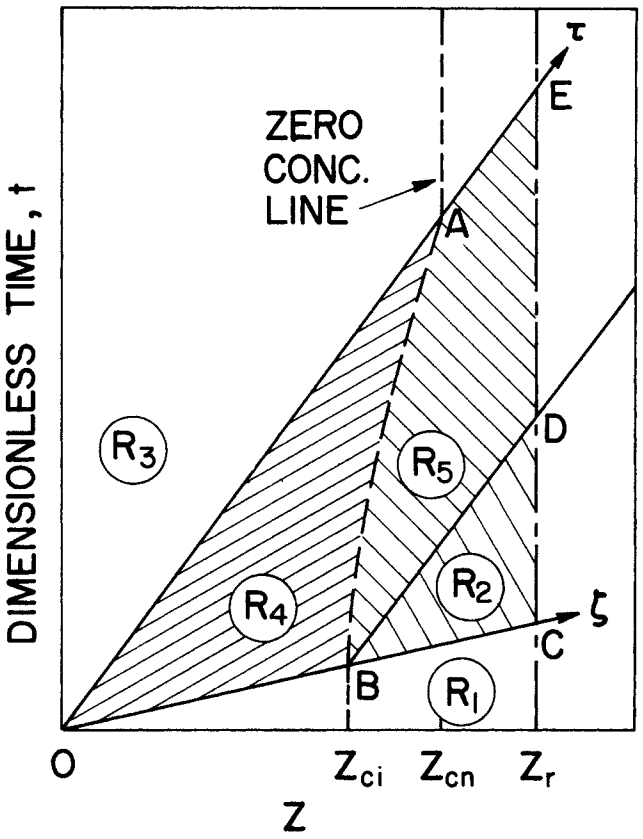

Figure 1. Various regions in the z-t plane for a sudden change in feed temperature.

Integration of Eqs. 5 and 6 for the adiabatic case gives (Douglas and Eagleton, 1962):

$$z = \exp(-\gamma)/\beta\{y \exp(\gamma/y) - y_o \exp(\gamma/y_o) + \gamma[Ei(\gamma/y_o) - Ei(\gamma/y)]\} \qquad n = 0 \tag{13a}$$

$$z = \exp(-\gamma)\{Ei(\gamma/y) - Ei(\gamma/y_o)\} - \exp(\gamma/(y_o + \beta))\left\{Ei\left[\frac{\gamma}{y} - \frac{\gamma}{(y_o + \beta)}\right] - Ei\left[\frac{\gamma}{y_o} - \frac{\gamma}{(y_o + \beta)}\right]\right\} \qquad n = 1, \tag{13b}$$

where the exponential integral Ei is defined as (Abramowitz and Stegun, 1971):

$$Ei(w) = -\int_{-w}^{\infty} \frac{\exp(-t)dt}{t}. \tag{14}$$

For a zeroth-order reaction in a cooled reactor, Eq. 10 gives:

$$z = \gamma/\beta \exp(-\gamma) F_1(U\gamma \exp(-\gamma)/\beta, y_w/\gamma, y/\gamma, y_o/\gamma) \tag{15}$$

where we define

$$F_1(a, b, w_2, w_1) \triangleq \int_{w_1}^{w_2} \frac{\exp(1/t)dt}{1 + a(b - t)\exp(1/t)}. \tag{16}$$

Eq. 13a is in fact a special case of Eq. 15. In order to determine z_c for a zeroth-order reaction, we find the value of y for which x vanishes. Dividing Eq. 5 by Eq. 6 and integrating yields:

$$\beta(1 - x) = \gamma F_o[U\gamma \exp(-\gamma)/\beta, y_w/\gamma, y/\gamma, y_o/\gamma] \tag{17}$$

where we define

$$F_o(a, b, w_2, w_1) \triangleq \int_{w_1}^{w_2} \frac{dt}{1 + a(b - t)\exp(1/t)} \tag{18}$$

In the adiabatic case $U = 0$ and

$$\beta(1 - x) = y - y_o. \tag{19}$$

It follows that z_c can be computed from Eq. 15, using either Eq. 17 or 19 to determine the value of y for which $x = 0$.

In the transient analysis of the zeroth-order case we shall use an extended steady-state profile, denoted by y_e. This is the dimensionless temperature profile computed from either Eq. 13a or 15 with $y_o = 1$, ignoring the fact that the concentration vanishes at $z = z_c$. Clearly, the initial and extended steady-state profiles are identical for all $z \leq z_c$.

Consider now a first-order reaction occurring in an adiabatic packed-bed reactor with intraparticle concentration gradients. When $\phi_o << 1$ $\eta \rightarrow 1$ and Eq. 13b is valid. For large diffusional resistances ($\phi_o >> 1$)

$$\eta \rightarrow \phi_o^{-1} \exp\left[-\frac{\gamma}{2}(1 - 1/y)\right] \tag{20}$$

and Eq. 13b can be still used if z is replaced by $z\phi_o^{-1}$ and γ is replaced by $\gamma/2$. In the intermediate range of ϕ_o where neither asymptotic form of η holds the temperature profile may be computed from

$$z = \int_{y_o}^{y} \frac{dy'}{(y_o + \beta - y')f(y')\eta(y', \phi_o)}. \tag{21}$$

In general $f\eta$ is a monotonic increasing function of y for all ϕ_o and η is a monotonic decreasing function of ϕ_o. Thus, the steady-state temperature at any fixed position in the reactor decreases as ϕ_o is increased. It also follows from Eq. 21 that at a fixed position the temperature in the initial steady state ($y_o = 1$) is higher than that in the new steady state ($y_o = \theta$).

Structure of the Transient Solutions

The hyperbolic Eqs. 2 and 3 may be solved by the method of characteristics (Aris and Amundson, 1973). This method enables the determination of all the qualitative features of the dynamic response without having to carry out any numerical computations.

We present here some background material concerning the nature of the solutions of Eqs. 2 and 3 in the (z, t) plane. This information will be utilized in the following sections to analyze the wrong-way behavior. As this behavior occurs only when the initial steady-state temperature increases with conversion, we restrict the analysis to such cases and ignore the uninteresting case in which the reactor is overcooled, so that the temperature is a monotonic decreasing function of z, i.e. when $F(1) < 0$.

We first replace the variables z and t by new variables ζ and τ defined so that

$$\frac{\partial t}{\partial \zeta} = \frac{1}{v_c} \tag{22a}$$

$$\frac{\partial z}{\partial \zeta} = \frac{\partial t}{\partial \tau} = \frac{\partial z}{\partial \tau} = 1. \tag{22b}$$

Applying these definitions and the chain rule, Eqs. 2 and 3 may be transformed into

$$\frac{\partial x}{\partial \zeta} = -x^n H(x) f(y)\eta(y, \phi_o) \tag{23}$$

$$\frac{\partial y}{\partial \tau} = \beta x^n H(x) f(y)\eta(y, \phi_o) + U(y_w - y). \tag{24}$$

Choosing the origin of the (ζ, τ) coordinates to coincide with the origin of the (z, t) coordinates, integration of Eq. 22 gives

$$z = \zeta + \tau \tag{25a}$$

$$t = \zeta/v_c + \tau. \tag{25b}$$

Setting ζ in Eq. 25 equal to a constant defines a family of temperature or y characteristics

$$t = z - \zeta_c(v_c - 1)/v_c. \tag{26}$$

Similarly, setting τ equal to a constant in Eq. 25 defines a family of concentration or x characteristics

$$t = z/v_c + \tau_c(v_c - 1)/v_c. \tag{27}$$

The speed of propagation of the concentration and temperature disturbances are represented by the inverse of the slopes of the x and y characteristics, respectively. For liquid-solid systems $v_c > 1$ while for gas-solid systems $v_c >> 1$.

The y and x characteristics passing through the point at which the step decrease in feed temperature occurs, are represented by the straight lines OAE and OBC in Figure 1. The region bounded by these two characteristics is the region of influence of the disturbance. In other words, the transient behavior due to the disturbance is limited to points bounded by OAE and OBC in the (z, t) plane.

In the region below OBC, denoted as R_1, the dimensionless concentration and temperature profiles are $x_i(z)$ and $y_i(z)$; while in the region above OAE, denoted as R_3, the concentration and temperature profiles are $x_n(z)$ and $y_n(z)$. It can be shown that the concentration profiles are continuous across the limiting characteristics OBC and OAE. However, because of the temperature jump at 0 the temperature is not continuous across the temperature characteristic OAE, but is continuous across the concentration characteristic OBC. The dashed line in Figure 1 is the locus of the points at which the concentration vanishes at any time $t > 0$ for a reaction of order less than unity. In this case it can be shown that the reactor length at which complete conversion is attained for the new steady state, z_{cn}, is larger than that corresponding to the initial steady state, z_{ci}. All the interesting dynamic responses occur in R_4 and R_5 in the (z, t) plane.

DYNAMICS OF ZEROTH-ORDER REACTION

We now examine the basic features of the transient solution by restricting the discussion to the zeroth-order reaction. We shall treat later the case of an adiabatic first-order reaction to illustrate the new behavioral features introduced by a reaction for which the reactants are not completely consumed. A unique feature of the zeroth-order reaction is that the transient temperature profiles may be constructed directly from the extended steady-state profiles. To illustrate this, consider two points T and T' in R_4 so that $z(T) = z(T')$. Let LT and $L'T'$ be two temperature characteristics passing through T and T', respectively (see Figure 2). Both L and L' are located at $z = 0$ and $t < 0$ so that $y(L) = y(L') = 1$. It follows from Eq. 24 that for any $x > 0$ y depends only on the initial condition and the length of the integration path so that $y(T) = y(T')$, and

$$\frac{\partial y(T)}{\partial t} = 0 \qquad T \text{ in } R_4. \tag{28}$$

For $z \leq z_{ci}$ the points with the same z in R_1 and R_4 have the same temperature. Stated differently, the transient temperature in this portion of R_4 is the same as that of the initial steady state. For $z > z_{ci}$ the temperature in R_4 is that of the extended steady state. Since the temperatures of the initial and extended steady states are the same for $z < z_{ci}$, we can state that the temperature at any point in R_4 is that of the extended steady state.

The temperature at any point J (see Figure 2) to the right of the zero concentration line is attained by integrating

$$\frac{\partial y}{\partial \tau} = U(y_w - y) \tag{29}$$

along the y characteristic passing through J which intersects the zero concentration line at K. For example, the temperature at point J in Figure 2 is given by

$$y(J) - y_w = [y(K) - y_w] \exp\{-U[\tau(J) - \tau(K)]\}. \tag{30}$$

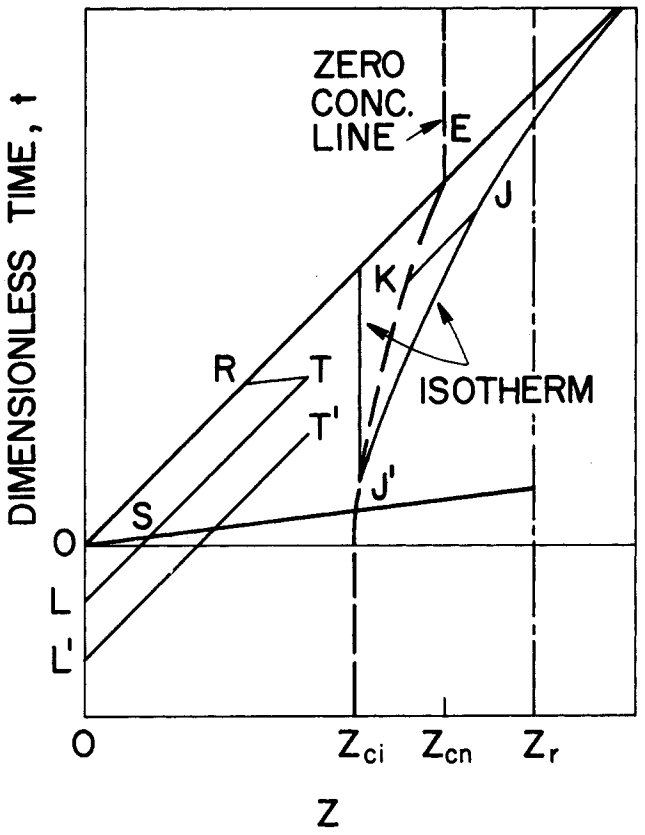

Figure 2. A schematic for the region of influence for a sudden change in feed temperature.

In the adiabatic case $U = 0$ and the temperature characteristics to the right of the zero concentration line are isotherms.

In the special case of a reaction which is completed in a finite length, the temperature characteristic BD and the concentration characteristic BC bound a region, denoted by R_2 in Figure 1, in which the concentration and temperature at any point is equal to that of a point in R_1 with the same z coordinate, i.e. that of the initial steady state. Thus, in R_2 $x = 0$ while y is given by $y_i(z)$. We prove in the appendix that for any point in R_4

$$\frac{\partial x}{\partial t} > 0, \tag{31}$$

and

$$\left(\frac{dt}{dz}\right)_x > 1. \tag{32}$$

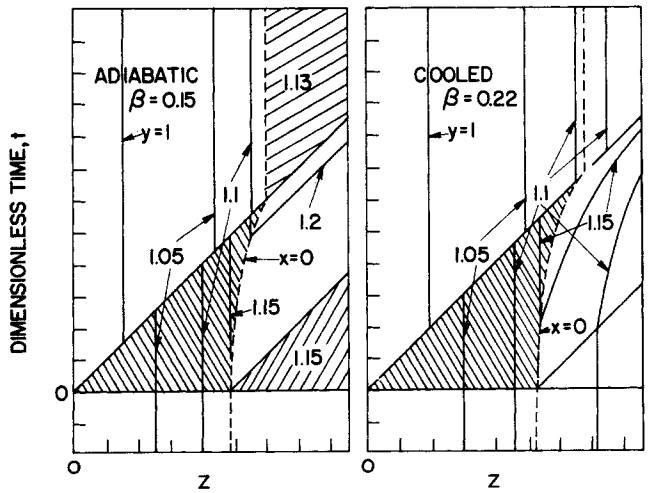

Figure 3. Isotherms for a zeroth-order reaction. Parameters are: $\gamma = 12$ and $\theta = 0.98$. For the cooled reactor $U = 1$ and $y_w = 0.9$.

Eq. 32 implies that any isoconcentration line, defined by the graph

$$x(z, t) = \text{constant}, \tag{33}$$

bends to the right with a slope exceeding that of the y characteristics. This guarantees that all the isoconcentration lines intersect any y characteristic. In particular, the line of zero concentration crosses the limiting concentration characteristic OC at some point B, say. It then bends to the right with a slope greater than unity and finally intersects the limiting temperature characteristic OE at point A. A simple numerical scheme for computing any isoconcentration line is presented in the appendix.

For a cooled reactor the temperature in R_5 decreases along a y characteristic and the y characteristics intersect successively cooler isotherms. Thus, the slopes of the isotherms must exceed the unity slope of the y characteristics. In the adiabatic case the y characteristics in R_5 are the isotherms. Figure 3 depicts the isotherms for the adiabatic and cooled reactors. An interesting feature of the cooled reactor is that within a steady-state region the isotherms may exist in two disjointed segments. The isotherm $y = 1.1$ in Figure 3 illustrates this behavior.

The regions in the (z, t) plane in Figure 1 were constructed without regard to the reactor length. For a reactor with a specific length (z_r, say) one needs to consider only the regions bounded between the vertical lines $z = 0$ and $z = z_r$ so that certain regions shown in Figure 1 may not exist. For example, if $z_r < z_{ci}$ then regions R_2 and R_3 do not exist.

We define the wrong-way behavior as a transient temperature rise which results from a sudden decrease in the feed temperature. Inspection of Figure 1 indicates that this behavior can occur only if the reactor is longer than z_{ci} as the temperature at any point in R_4 with $z \leq z_{ci}$ is that of the initial steady state.

Limiting Transient-Peak Temperature

The highest temperature in the (z, t) plane occurs at the right-most point in R_4, A, where $z = z_{cn}$. This limiting transient-peak temperature will be denoted by y_p. It may be determined by substitution of the value of z_{cn} into Eq. 13a or 15 which describe the extended steady state. For an adiabatic reactor y_p is the solution of

$$(\beta + \theta) \exp [\gamma/(\beta + \theta)] - \theta \exp (\gamma/\theta) + \gamma\{Ei(\gamma/\theta) - Ei[\gamma/(\beta + \theta)]\} = y_p \exp (\gamma/y_p) - \exp (\gamma) + \gamma[Ei(\gamma) - Ei(\gamma/y_p)]. \tag{34}$$

In this case, y_p depends only on the dimensionless activation energy γ, adiabatic temperature rise β, and new feed temperature θ. The analogous expression for the cooled reactor is

$$F_1(U\gamma \exp (-\gamma)/\beta,\ y_w/\gamma,\ y_{cn}/\gamma,\ \theta/\gamma) = F_1(U\gamma \exp (-\gamma)/\beta,\ y_w/\gamma,\ y_p/\gamma,\ 1/\gamma) \tag{35}$$

Here y_p depends on the dimensionless heat transfer capacity U and wall temperature y_w in addition to γ, β and θ. In an adiabatic reactor $y_p > 1 + \beta$. No similar lower bound exists for the cooled reactor.

For any reactor with $z_r \geq z_{cn}$ the limiting transient-peak temperature is attained at $z = z_{cn}$ in a cooled reactor and at all the points in (z_{cn}, z_r) in an adiabatic reactor. For any reactor with length $z_{ci} < z_r < z_{cn}$ a temperature greater than $y_i(z_{ci})$ but less than y_p will occur at some time for all the points for which $z > z_{ci}$. The highest transient temperature occurs at the outlet of the reactor and is equal to that of the extended steady state as computed by either Eq. 13a or 15 with $z = z_r$. Examples illustrating the development of the transient temperature rise will be presented in the next section.

We have seen that the wrong-way behavior occurs only if $z_r > z_{ci}$. The highest transient temperature can be computed from

Eq. 13a or 15 if $z_{ci} < z_r < z_{cn}$ or from Eq. 34 or 35 if $z_r > z_{cn}$. The use of Eq. 13a or 34 for computing the highest temperature in an adiabatic reactor is rather convenient since tables of the exponential integral are available. However, tables of F_0 and F_1 are not available and we shall now describe a more convenient approach for computing the limiting transient-peak temperature in a cooled reactor.

For $z = z_{cn}$ Eq. 10 gives

$$\beta z_{cn} = \int_1^{y_p} \frac{dy'}{F(y')} = \int_\theta^{y_{cn}} \frac{dy'}{F(y')}. \tag{36}$$

Differentiating Eq. 36 with respect to θ and rearranging gives

$$\frac{dy_p}{d\theta} = F(y_p)\left[\frac{1}{F(y_{cn})}\frac{dy_{cn}}{d\theta} - \frac{1}{F(\theta)}\right]. \tag{37}$$

Since $x_p = 0$ at $z = z_{cn}$ Eq. 17 becomes

$$\beta = \int_\theta^{y_{cn}} \frac{f(y')dy'}{F(y')}. \tag{38}$$

Differentiation of Eq. 38 with respect to θ yields

$$\frac{dy_{cn}}{d\theta} = \frac{f(\theta)F(y_{cn})}{F(\theta)f(y_{cn})}. \tag{39}$$

Substitution of Eq. 39 into 37 gives

$$\frac{dy_p}{d\theta} = \frac{F(y_p)}{F(\theta)}\left[\frac{f(\theta)}{f(y_{cn})} - 1\right]. \tag{40}$$

In the special case of an adiabatic reactor $f(y) = F(y)$ and $y_{nc} = \theta + \beta$ which gives

$$\frac{dy_p}{d\theta} = f(y_p)\left[\frac{1}{f(\theta+\beta)} - \frac{1}{f(\theta)}\right] = e^{-\gamma/y_p}[e^{\gamma/(\theta+\beta)} - e^{\gamma/\theta}]. \tag{41}$$

Eq. 41 may be integrated numerically to get graphs of y_p vs. θ of the type displayed in Figures 4 and 5. Eq. 41 may also be integrated analytically to obtain the implicit Eq. 34. For a cooled reactor the relation between y_{cn} and θ is not simple, and Eqs. 39 and 40 need to be solved simultaneously to get the y_p vs. θ graphs. It will be proven later that Eqs. 34 and 41 can be used to predict the limiting transient-peak temperature for any n-th order reaction in an adiabatic reactor.

Figures 4 and 5 show that y_p increases slowly with decreasing θ close to unity. However, when θ becomes smaller than a certain critical value θ^*, y_p increases very rapidly to unrealistically high values. This indicates that beyond θ^* additional physical phenomena not included in this simple model, must become significant and decrease the limiting transient-peak temperature. It is interesting to note that for sufficiently small θ, i.e. for sufficiently large reduction in the feed temperature, the limiting transient-peak temperature attained in a cooled reactor is higher than that attained in an adiabatic reactor in which the same reaction is carried out. Thus, the cooling may increase the transient temperature excursion following a rapid decrease in the feed temperature.

The graphs suggest that potential problems are associated with a rapid decrease in the feed temperature, and that the transient-peak temperature may be high enough to damage the catalyst or to initiate dormant side reactions.

Graphical Construction of Transient Temperature Profiles

It is of practical interest to know in addition to the peak temperature the shape of the temperature profiles at various times and the temperature histories at several points. For the case of a zeroth-order reaction this information can be determined by a simple graphical scheme using the (z, t) plane and the new and extended steady-state profiles. This scheme will be illustrated by means of Figure 6.

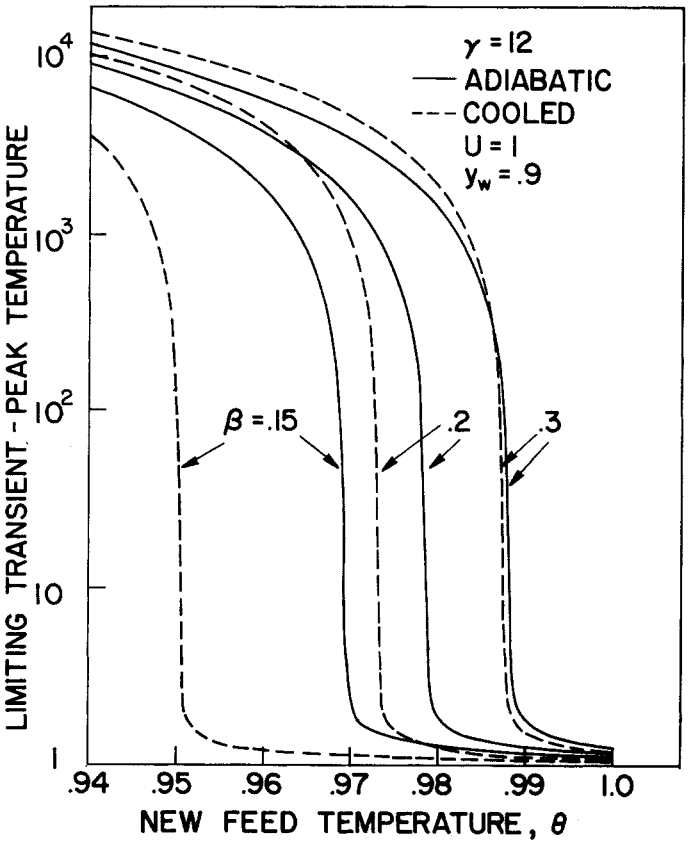

Figure 4. Dependence of the limiting peak temperature on θ for various values of the dimensionless adiabatic temperature rise at $\gamma = 12$.

The upper part of Figure 6 is a representation of the (z, t) plane with OPA and OBC bounding the region of influence of the sudden disturbance. Due to the high value of v_c the charac-

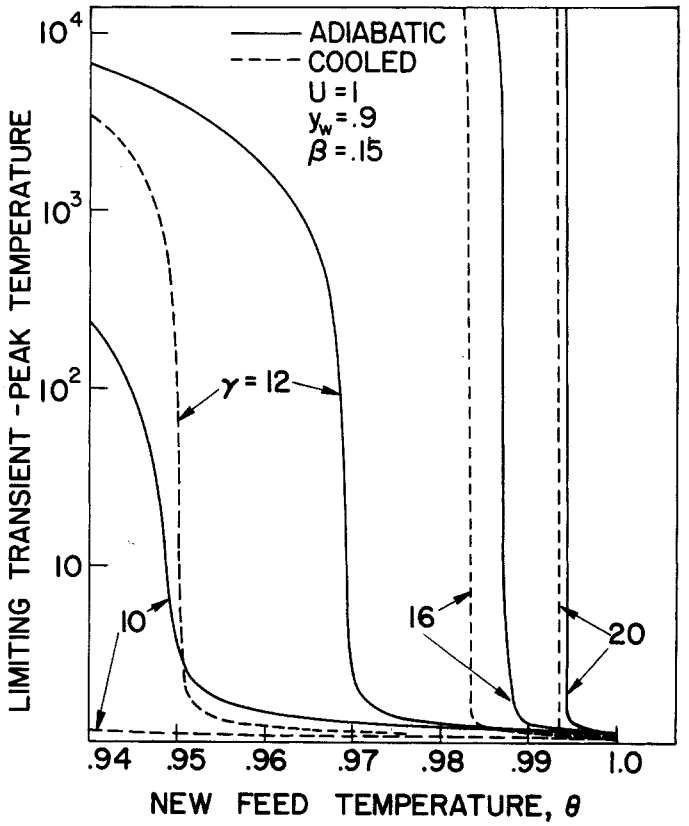

Figure 5. Dependence of the limiting peak temperature on θ for various values of the dimensionless activation energy at $\beta = 0.15$.

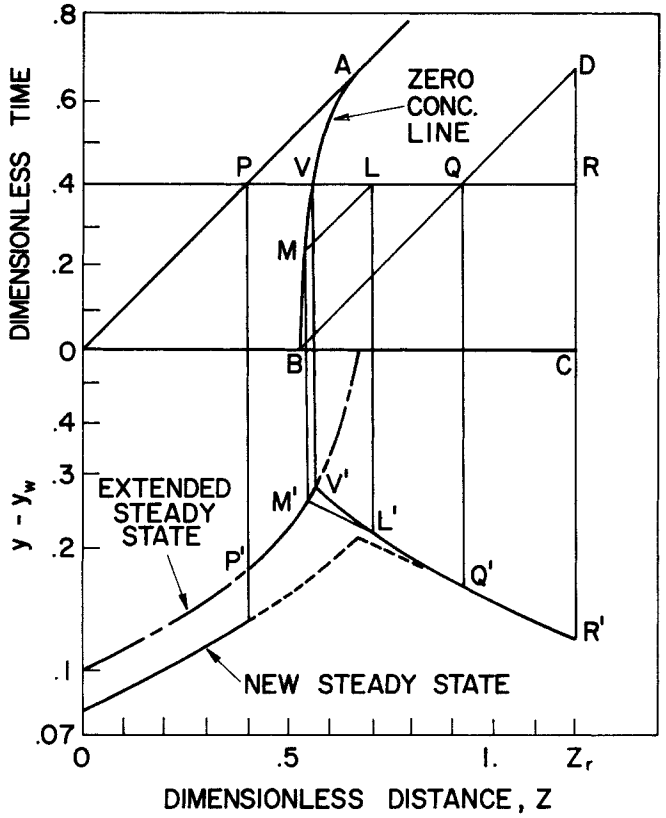

Figure 6. Graphical construction of a transient temperature profile for a zeroth-order reaction in a cooled reactor.

teristic OBC is indistinguishable from the z axis. The lower portion of Figure 6 includes the profiles $y_e - y_w$ and $y_n - y_w$ on a logarithmic scale.

Suppose the profile at a time t is desired. The horizontal line $t = \bar{t}$ intersects OPA at P, the line of zero concentration at V, the line BD at Q and the line $z = z_r$ at R. Let L denote an arbitrary point on VQ and M be the point where the y characteristic through L intersects the line of zero concentration. A primed letter denotes a point in the bottom portion of Figure 6 corresponding to the one denoted by the same letter in the top portion of the figure.

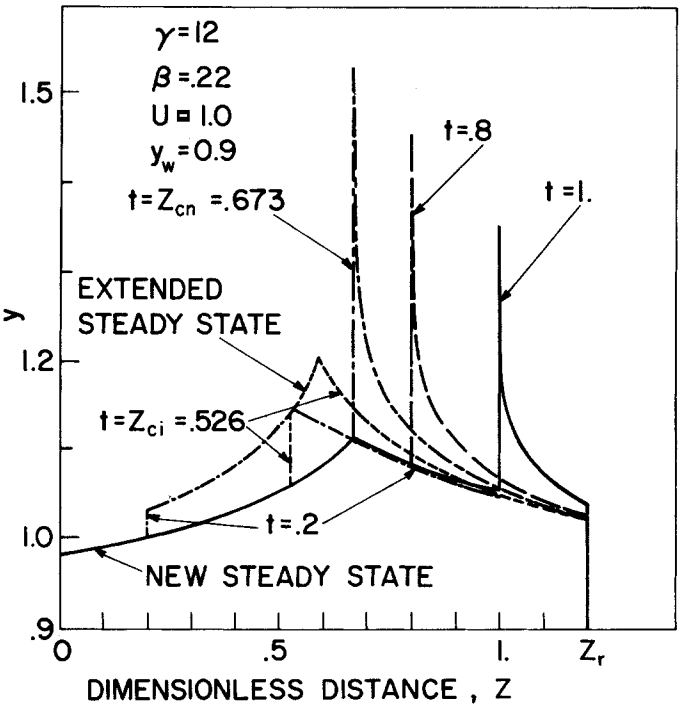

Figure 8. Transient temperature profiles for a zeroth-order reaction in a cooled reactor with $\theta = 0.98$.

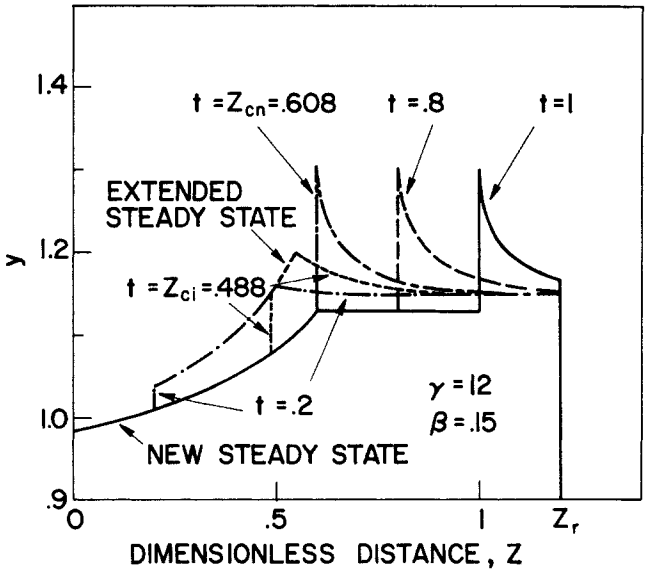

Figure 7. Transient temperature profiles for a zeroth-order reaction in an adiabatic reactor with $\theta = 0.98$.

For all $z < z(P)$ the transient profile is the same as the new steady state. At P, the temperature jumps to that of the extended steady-state profile. For all the points between P and V the transient profile is the same as the extended steady-state profile, so that the highest temperature at time t is attained at V. In the region between V and Q the temperature decreases exponentially from its value at V. Thus, at a point L in (V, Q)

$$ln(y(L) - y_w) = ln(y(M) - y_w) - U[z(L) - z(M)]. \quad (42)$$

The graphical solution of Eq. 42 is accomplished by drawing a vertical line from M intersecting the extended steady state at M'. The intersection of a line with a slope of $-U$ through M' with a vertical line through L determines L', the desired point on the transient temperature profile. For any point in (Q, R) the temperature is equal to that of the initial steady state. A similar procedure may be used to determine the concentration profile using the new and extended steady-state profiles (Mehta, 1978).

The same graphical scheme may be used for an adiabatic reactor with y_w being any convenient reference temperature and the slope of $M'L'$ being zero. A simpler scheme is to plot in the lower portion of Figure 6 y_e and y_n on a linear scale and to use the same procedure as before.

Figure 7 illustrates the temperature profiles in an adiabatic reactor. A temperature jump is always attained at the point corresponding to the intersection of the line $t = \bar{t}$ with the y characteristic OA. The peak develops in the region $z > z_{ci}$ and becomes fully developed for $t = z_{cn}$. For all times $t \geq z_{cn}$ the temperature profile jumps directly from the new steady state to y_p without an intervening segment from the extended steady state, and this completely developed peak moves downstream without a change in shape at a constant velocity of 1. After one thermal residence time ($t = z_r$) the peak exits the reactor and the new steady state is attained.

In the cooled reactor (Figure 8), a temperature peak exists at $z = z_{ci}$ in the initial steady state. During the transient period this peak sharpens and moves downstream. At $t = z_{cn}$, the peak attains its maximum amplitude and is located at $z = z_{cn}$. For $z_{cn} < t < z_r$ two temperature peaks exist. The first peak corresponds to the peak in the new steady state at $z = z_{cn}$. This is followed by a decay for $z_{cn} < z < t$ and a jump to the primary peak at $z = t$. The primary peak propagates downstream with decreasing amplitude and leaves the reactor after one thermal residence time.

The behavior of the temperature at a fixed point can be determined by examining either Figure 1 or 3. Consider first the

adiabatic reactor. For $z < z_{ci}$ the temperature remains in the initial steady state, $y_i(z)$, until $t = z$. It then drops to the new steady-state value, $y_n(z)$. For $z_{ci} < z < z_{cn}$ the temperature remains at $1 + \beta$ in region R_2. The temperature rises with time in R_5 and reaches its maximum value, $y_e(z)$, at the boundary between R_4 and R_5. The temperature remains at this value until $t = z$. It then drops to the final value, $y_n(z)$. For $z > z_{cn}$ the behavior is similar to the preceding case, but there exists no period during which the temperature remains constant at its maximum value.

In a cooled reactor the qualitative behavior of the temperature at a fixed point is similar to that in an adiabatic reactor, and the preceding discussion is valid with the exception that in R_2 the constant temperature $y_i(z)$ is less than $1 + \beta$. It is of interest to note that in an adiabatic reactor the new steady-state temperature at any point is lower than the initial temperature. However, in a cooled reactor the local steady-state temperature may increase upon a decrease in the feed temperature in a region close to the exit. This behavior may lead to a control action in the wrong direction and complicates the development of rational control policies for the reactor.

The concentration at any fixed point $z < z_{cn}$ remains at its initial value, $x_i(z)$, until R_4 is reached. The concentration then increases according to Eq. A11 until it reaches the final value of $x_n(z)$ at $t = z$. The concentration for $z \geq z_{cn}$ is zero for all times.

A FIRST-ORDER REACTION IN AN ADIABATIC REACTOR

A first-order reaction is an example of one for which the reactant is not completely consumed in a reactor of finite length. Therefore the zero concentration line and regions R_2 and R_5 do not exist in this case. The transient analysis of the first-order reaction is more complex than that of the zeroth-order reaction since Eqs. 2 and 3 remain coupled within R_4. In the appendix we show that

$$\frac{dy(T)}{dt} > 0 \qquad T \text{ in } R_4. \tag{43}$$

Thus, in contrast with the zeroth-order case the isotherms in R_4 are not vertical. In order to study the behavior of the isotherms in more detail use is made of the equation

$$\frac{\partial y}{\partial \zeta} = f(y)\eta(y, \phi_o)\,[1 + \beta - y] \tag{44}$$

which is derived in the appendix. Starting at a point R on OE (see Figure 2), Eq. 44 can be integrated along an x characteristic to obtain the temperature at any point T in R_4. If $y(R_-) < 1 + \beta$, then y increases along the characteristic and asymptotically approaches $1 + \beta$. If $y(R_-) = 1 + \beta$, then $\partial y/\partial\zeta$ is zero, and the x characteristic is the $1 + \beta$ isotherm. If $y(R_-) > 1 + \beta$, y decreases along the characteristic and asymptotically approaches $1 + \beta$. Since the temperature increases monotonically along OE, the point on OE where $y = 1 + \beta$ is unique. This point is denoted by M in Figure 9.

The x characteristic through M which is the $1 + \beta$ isotherm is denoted by MN. This isotherm is referred to as the critical isotherm since it divides R_4 into two regions. In the region below MN denoted R_{4a} the temperature is lower than $1 + \beta$ and in the region above MN, which is called R_{4b}, the temperature is higher than $1 + \beta$. The z coordinate of point M is called the critical reactor length and is denoted by z_{cr}. The isotherms must be vertical as they cross OC because of continuity. According to Eq. 43, the isotherms in R_{4a} bend to the left and terminate on OM since the temperature for any isotherm which intersects OC is lower than $1 + \beta$. Since $\partial y/\partial\zeta < 0$ in R_{4b}, the x characteristics must cross successively cooler isotherms so that the slope of the isotherms in R_{4b} is greater than $1/v_c$, the slope of the x characteristics. Likewise, since $\partial y/\partial\tau > 0$ the slope of the isotherms must be less than unity, the slope of the y characteristics. Figure 9 portrays the isotherm pattern in R_4.

In the case of negligible diffusion resistance Eq. 44 can be integrated analytically to determine y in R_{4a} from

$$Ei(\gamma/y(T)) - \exp\left(\frac{\gamma}{1+\beta}\right)Ei\left[\gamma\left(\frac{1}{y(T)} - \frac{1}{1+\beta}\right)\right] = \zeta \exp(\gamma) + Ei(\gamma/y(R_-)) - \exp\left(\frac{\gamma}{1+\beta}\right)Ei\left[\gamma\left(\frac{1}{y(R_-)} - \frac{1}{1+\beta}\right)\right], \tag{45}$$

and in R_{4b} from

$$Ei(\gamma/y(T)) - \exp\left(\frac{\gamma}{1+\beta}\right)E_1\left[\gamma\left(\frac{1}{1+\beta} - \frac{1}{y(T)}\right)\right] = \zeta \exp(\gamma) + Ei(\gamma/y(R_-)) - \exp\left(\frac{\gamma}{1+\beta}\right)E_1\left[\gamma\left(\frac{1}{1+\beta} - \frac{1}{y(R_-)}\right)\right] \tag{46}$$

where E_1 is defined as (Abramowitz and Stegun, 1971)

$$E_1(w) = \int_1^\infty \frac{\exp(-wt)}{t}\,dt. \tag{47}$$

In the case of a large diffusional resistance Eqs. 45 and 46 may be used by replacing ζ by $\zeta\phi_o^{-1}$ and γ by $\gamma/2$ according to Eq. 20. In the intermediate case the temperature at T is obtained by integrating Eq. 44 numerically. If $y(R_-) \neq 1 + \beta$ then $x(T)$ can be obtained from the following expression proved in the appendix

$$\frac{y(T) - (1+\beta)}{y(R_-) - (1+\beta)} = \frac{x(T)}{x(R)}. \tag{48}$$

If $y(R_-) = 1 + \beta$ then

$$x(T) = x(R) \exp[-f(1+\beta)\eta(1+\beta, \phi_o)\zeta]. \tag{49}$$

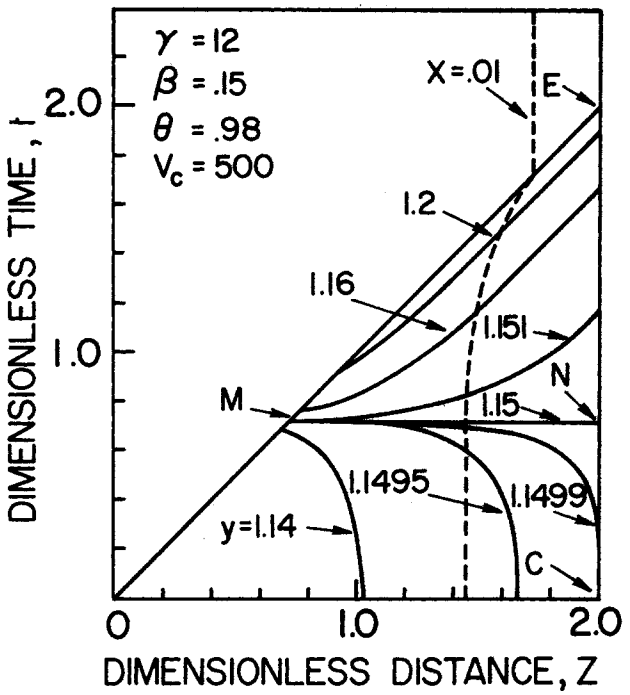

Figure 9. Isotherms for a first-order reaction in an adiabatic reactor.

Temperature Along OE

The maximum temperature at a fixed location z occurs at the intersection of the vertical line $z = \bar{z}$ with the limiting characteristic OE, since $\partial y/\partial t > 0$ in R_4. The maximum temperature along OE, i.e. the highest transient temperature in the adiabatic reactor occurs at the reactor exit, E. This is in contrast with the zeroth-order case in which the maximum temperature exists over a finite interval (z_{cn}, z_r) in an adiabatic reactor. An expres-

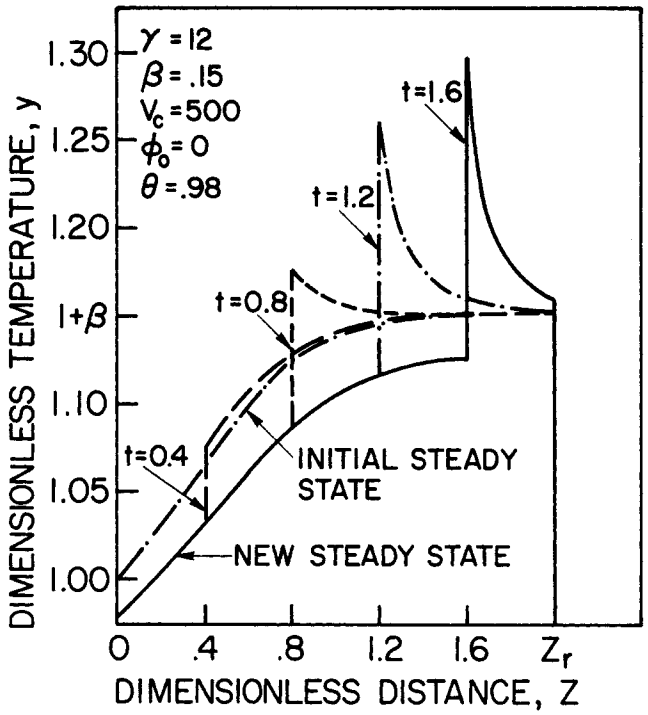

Figure 10. Transient temperature profiles for a first-order reaction in an adiabatic reactor with negligible diffusional resistance.

sion determining the maximum possible temperature along OE in an adiabatic reactor in which a reaction with separable kinetics occurs is obtained by writing Eq. 24 immediately to the right of OE

$$\frac{dy_-}{d\tau} = \beta g(x_n) G(y_-) H(x_n) \tag{50}$$

$$y_-(0) = 1, \tag{51}$$

and to the left of OE

$$\frac{dy_n}{d\tau} = \beta g(x_n) G(y_n) H(x_n) \tag{52}$$

$$y_n(0) = \theta, \tag{53}$$

where $g(x)$ and $G(y)$ are the concentration and temperature dependences of the separable rate expression, and we use the

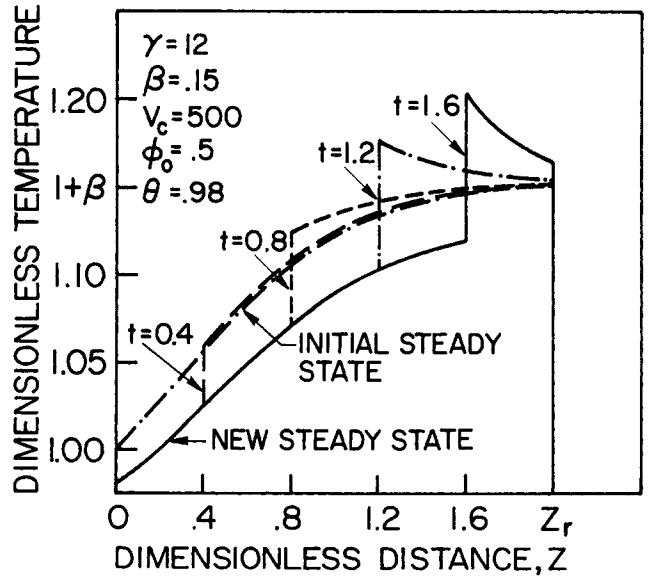

Figure 11. Transient temperature profiles for a first-order reaction in an adiabatic reactor accounting for intraparticle diffusional resistance.

fact that x is continuous across OE. Division of Eq. 50 by Eq. 52 gives

$$\frac{dy_-}{dy_n} = G(y_-)/G(y_n) \tag{54}$$

$$y_-(y_n = \theta) = 1. \tag{55}$$

Separating variables and integrating yields

$$\int_1^y \frac{dy'}{G(y')} = \int_\theta^{y_n} \frac{dy'}{G(y')}. \tag{56}$$

Differentiating Eq. 56 with respect to θ gives

$$\frac{dy}{d\theta} = G(y)\left[\frac{1}{G(y_n)}\frac{dy_n}{d\theta} - \frac{1}{G(\theta)}\right]. \tag{57}$$

If the reaction is completed in a finite length, then y_p can be computed from Eq. 57 by setting y_n equal to its maximum value of $\theta + \beta$. When $G(y)$ is of the Arrhenius form Eq. 57 becomes Eq. 41. Thus, Eq. 41 and its integrated form Eq. 34 can be used to compute y_p for any n-th order reaction in an adiabatic reactor. When the reactant is not completely consumed in a finite length, y_n approaches asymptotically $\theta + \beta$ for a very long reactor, and the temperature computed by Eq. 57 is an upper limit on the highest temperature in the reactor. The closeness of the approach to y_p depends on the length of the reactor and on $g(x)$. For a first-order reaction with diffusional resistance Eq. 41 is again obtained for either negligible or large diffusional resistances. In the latter case γ is replaced by $\gamma/2$.

$G(y)$ is a monotonic increasing function of y. Thus, it follows from Eq. 54 that

$$[y] \triangleq y_-(R) - y_n(R) > 1 - \theta, \tag{58}$$

that is the temperature jump across OE is larger than the step jump in the feed temperature. When $G(y)$ is of the Arrhenius form Eq. 54 can be integrated analytically to give

$$y_-(R) \exp\left(\frac{\gamma}{y_-(R)}\right) - \gamma Ei\left(\frac{\gamma}{y_-(R)}\right) = y_n(R) \exp\left(\frac{\gamma}{y_n(R)}\right) - \gamma Ei\left(\frac{\gamma}{y_n(R)}\right) + \gamma\{Ei(\gamma/\theta) - Ei(\gamma) + \gamma^{-1}\exp(\gamma) - \theta \exp(\gamma/\theta)\}. \tag{59}$$

Structure of Transient Temperature Profiles

For a first-order reaction the transient temperature at any fixed point increases with time in R_4 according to Eq. 43. Thus, a wrong-way response occurs irrespective of the reactor length. The transient temperature exceeds the original adiabatic temperature of $1 + \beta$ only in R_{4b}. Therefore, a temperature excursion of $y > 1 + \beta$ occurs only for sufficiently long reactors, i.e., $z_r > z_{cr}$.

Unlike the case of a zeroth-order reaction, the transient temperature profiles cannot be constructed graphically, but are obtained by solving either the differential Eqs. 6, 54, and 44 or the implicit Eqs. 13a, 59, 45, and 46 for y_n, $y_-(R)$, and $y(T)$. The concentration is then found from Eq. 19, 48, or 49. Figures 10 and 11 portray the transient temperature profiles for various times. Figure 10 is drawn for the case of negligible diffusion resistance. Figure 11 is for $\phi_0 = 0.5$ with all other parameters the same as in Figure 10. For $z < t$ the temperature profile follows the new steady state. At $z = t$ the temperature jumps to $y_-(t)$ which is higher than $y_i(t)$. For small values of t the temperature increases monotonically with increasing axial position for points to the right of the jump, e.g. $t = 0.4$ in Figure 10 and $t = 0.4$ and 0.8 in Figure 11. For large t the temperature to the right of the jump decreases with axial position resulting in a peak in the temperature profile. Since the right hand side of Eq. 54 is greater than unity, the magnitude of the temperature discontinuity increases with time. Thus, as the discontinuity propagates down the reactor it simultaneously becomes larger in

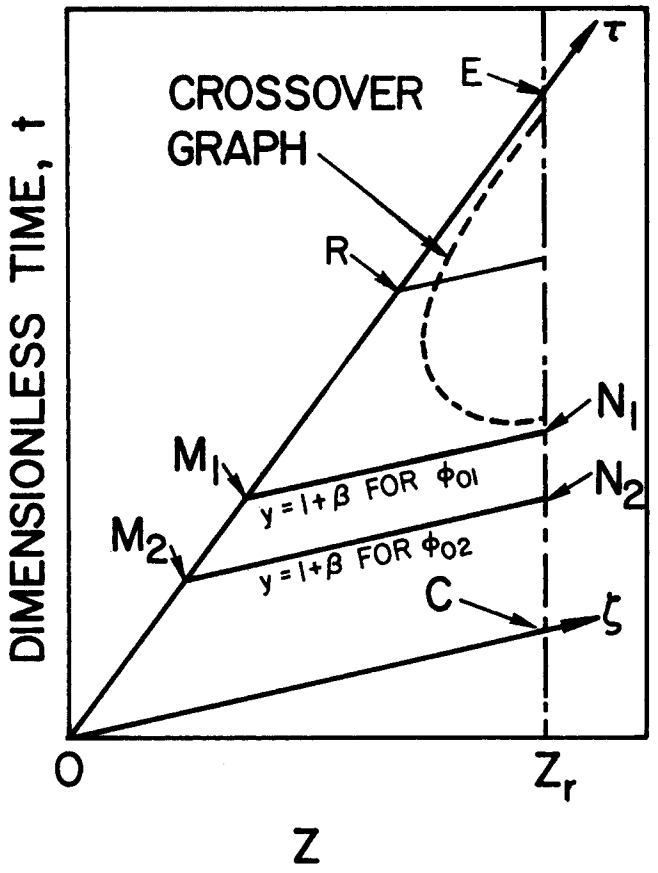

Figure 12. The critical isotherms for two different Thiele moduli and a schematic of the corresponding crossover graph.

magnitude and develops a peaked shape. The diffusional resistance delays the development of the peak relative to the case of negligible resistance (compare the profiles for $t = 0.8$ in Figures 10 and 11) and lowers the peak temperature. For all $t > z_r/v_c$ the transient profile approaches the initial steady-state profile downstream from the discontinuity. If $t < z_r/v_c$ then y_i persists for $z > v_c t$. The concentration is continuous along $t = \bar{t}$ but a discontinuity in dx/dz occurs at the intersection with OE.

The temperature and concentration variation at a fixed z are as follows. For $t < z/v_c$ the temperature and concentration remain at their initial steady-state values, $y_i(z)$ and $x_i(z)$. At $t = z/v_c$ the temperature and concentration begin to rise and reach their maximum values, $y_-(z)$ and $x_n(z)$, at $t = z$. The temperature then drops to $y_n(z)$ while the concentration remains at $x_n(z)$.

Transient Temperature Increase by Diffusional Limitation

It has already been pointed out that increasing ϕ_o decreases the steady-state temperature at a fixed point in the reactor. In the appendix it is shown that the same behavior occurs along OE during the transient period, so that

$$y_-(R, \phi_{01}) < y_-(R, \phi_{02}) \tag{60}$$

if

$$\phi_{01} > \phi_{02}. \tag{61}$$

The maximum temperature occurs at E and Eq. 60 implies that increasing ϕ_o decreases the highest transient temperature. We now examine whether $y(T, \phi_{01}) < y(T, \phi_{02})$ for all points T in R_4, i.e. whether increasing ϕ_{01} decreases the temperature everywhere in the (z, t) plane. Consider a point T in R_4 for two reactors with Thiele moduli ϕ_{01} and ϕ_{02} which satisfy Eq. 61. For each reactor a critical isotherm M_iN_i exists, and according to Eq. 60 M_1N_1 must lie above M_2N_2 (see Figure 12). If T lies in the region between M_1N_1 and M_2N_2 then

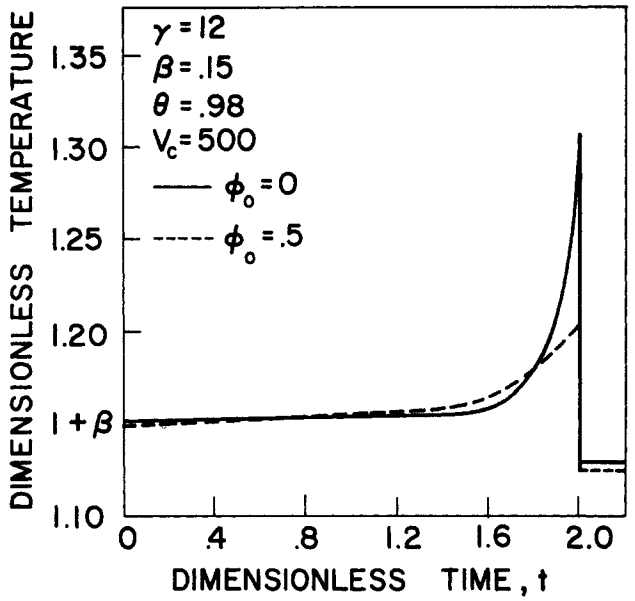

Figure 13. The crossover effect at the reactor exit ($z = 2.0$).

$$y(T, \phi_{01}) < 1 + \beta < y(T, \phi_{02}). \tag{62}$$

If T lies below M_2N_2 then

$$y(T, \phi_{01}) < y(T, \phi_{02}) \tag{63}$$

because of Eqs. 44, 60 and

$$\eta(y, \phi_{01})\,[1 + \beta - y] < \eta(y, \phi_{02})\,[1 + \beta - y]. \tag{64}$$

If T lies above M_1N_1 then $y > 1 + \beta$ and

$$0 > \eta(y, \phi_{01})\,[1 + \beta - y] > \eta(y, \phi_{02})\,[1 + \beta - y]. \tag{65}$$

Thus, starting at R, $y(T, \phi_{02}) > y(T, \phi_{01})$, but $y(T, \phi_{02})$ decreases more rapidly than $y(T, \phi_{01})$ along an x characteristic. It can be shown that a point exists such that $y(T, \phi_{02}) = y(T, \phi_{01})$ (Mehta, 1978). We define a crossover graph as the locus of

$$y(T, \phi_{01}) = y(T, \phi_{02}). \tag{66}$$

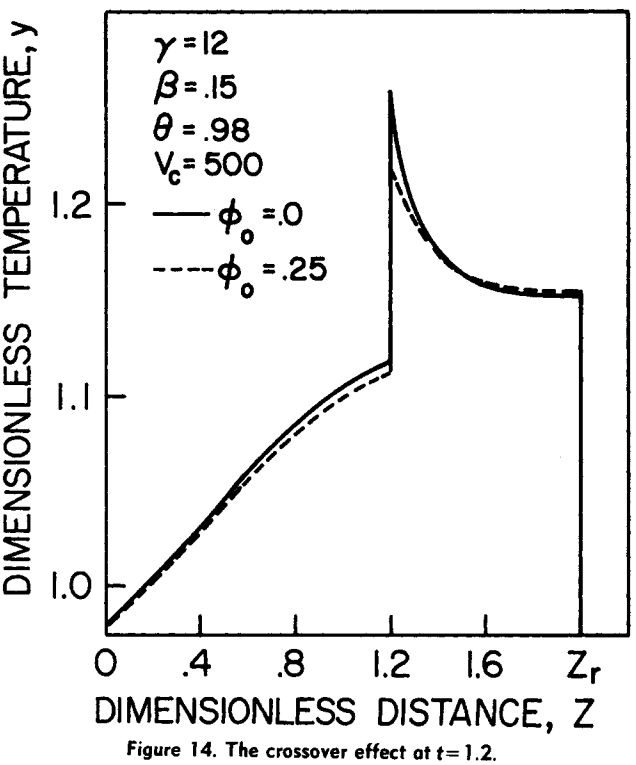

Figure 14. The crossover effect at $t = 1.2$.

In the region of the (z, t) plane to the right of the crossover graph the temperature in the reactor with the larger diffusional resistance exceeds that in the one with the smaller diffusional resistance.

Figures 13 and 14 illustrate the crossover effect. In Figure 13 the temperature-time variations at the reactor exit for $\phi_o = 0$ and $\phi_o = 0.5$ are compared. While in both cases $y_i(z_r) \simeq 1 + \beta$ the transient-peak temperature for $\phi_o = 0$ is considerably higher. However, during the time interval from approximately 0.8 to 1.8 the temperature for $\phi_o = 0.5$ is higher, i.e. there is a period of time prior to the arrival of the peak during which the diffusional resistance raises the temperature. In Figure 14 the fixed time variation of the temperatures for $\phi_o = 0$ and $\phi = 0.25$ are compared. Again the peak temperature for $\phi_o = 0$ is higher, but there exists a region downstream from the peak in which the temperature for $\phi_o = 0.25$ is higher. The graphs indicate that increasing the diffusional limitations lowers the transient-peak temperature and makes the response more sluggish. The graphs also show that during part of the transient period a crossover behavior occurs, and the temperature in the reactor with the larger diffusional limitation can exceed that in the one with the lower diffusional resistance.

CONCLUDING REMARKS

The analysis indicates that a large temperature excursion may be caused by a sudden decrease in the feed temperature. This transient temperature rise may damage the catalyst, initiate dormant undesired side reactions, and lead to a runaway. Thus, rapid temperature changes should be avoided in any packed-bed reactor control and shut-down procedure. When a failure in a preheater can cause a sudden drop in the feed temperature, such as a furnace failure in a hydrocracker, special control policies need to be devised to avoid the development of a large transient temperature peak.

The analysis indicates that high transient temperatures develop only in sufficiently long reactors. In the case of a zeroth-order reaction no temperature rise occurs unless $z > z_{ci}$ and the temperature peak is fully developed only if $z \geq z_{cu}$. For a first-order reaction the temperature does not exceed $1 + \beta$ unless $z > z_{cr}$. Thus, the impact of the wrong-way behavior is not encountered in short reactors.

The use of a pseudo-homogeneous model and either a zeroth or first-order reaction enables the determination of the complete structure of the dynamic behavior without having to perform any numerical computations. Moreover, in the zeroth-order case the exact dynamic response can be determined directly from the extended and new steady-state profiles.

The analysis gives valuable insight into the wrong-way behavior and points out the key parameters responsible for this dynamic response. While the model and the kinetics are the simplest one can use, the results serve as a useful baseline against which the predictions of more detailed and complex models can be compared. In a forthcoming publication we shall discuss the modified features which are introduced by more refined models and by assuming that the temperature change is not instantaneous.

The plug-flow pseudo-homogeneous model may introduce erroneous predictions in two situations. The first is when steady-state multiplicity exists so that the wrong-way behavior may lead to either ignition or extinction of the reactor. The simple model is not capable of predicting steady-state multiplicity and fails to predict this potential impact of the wrong-way behavior. This deficiency may be overcome by modifying the model so that it can predict the steady-state multiplicity. One possibility is to account for the axial dispersion of energy in the reactor.

Another prediction of the model, which violates physical intuition, is that the highest transient temperature is independent of v_c, the ratio between the propagation speed of the concentration and temperature disturbances. When v_c is close to unity, as may be the case when the fluid is a liquid or a gas at very high pressure, the domain of influence of the perturbation at the origin is very narrow, and the model predicts that extremely fast temperature changes occur. Under these conditions, the heat transfer resistance between the fluid and the solid particles and the axial dispersion of energy are expected to reduce considerably the peak temperature from the value predicted by the simple model.

ACKNOWLEDGMENT

This work was supported by the National Science Foundation.

APPENDIX

a. A Proof of Eqs. 31 and 32

Using Eq. 22 we get:

$$\frac{\partial \phi}{\partial \zeta} = \frac{1}{v_c}\frac{\partial \phi}{\partial t} + \frac{\partial \phi}{\partial z} \tag{A1}$$

$$\frac{\partial \phi}{\partial \tau} = \frac{\partial \phi}{\partial t} + \frac{\partial \phi}{\partial z}. \tag{A2}$$

Subtracting Eq. A1 from A2

$$\frac{\partial \phi}{\partial t} = \left(\frac{v_c}{v_c - 1}\right)\left(\frac{\partial \phi}{\partial \tau} - \frac{\partial \phi}{\partial \zeta}\right). \tag{A3}$$

For $n = 0$ and $\eta = 1$, Eq. 23 becomes

$$\frac{\partial x(T)}{\partial \zeta} = -f(y) \qquad T \text{ in } R_4. \tag{A4}$$

Consider an x characteristic between R and T (Figure 2). Integration of Eq. A4 gives

$$x(T) = x(R) - \int_{R_-}^{T} f(y)d\zeta. \tag{A5}$$

Note that the concentration is continuous at R so that $x(R_-) = x(R_+) = x_n(R)$. Where R_+ and R_- indicate that the limit is to be taken from the left and right, respectively. Differentiation of Eq. A5 with respect to τ gives

$$\frac{\partial x(T)}{\partial \tau} = \frac{\partial x_n(R)}{\partial \tau} - \int_{R_-}^{T} \frac{\partial f}{\partial \tau}\, d\zeta. \tag{A6}$$

But

$$\frac{\partial x_n(R)}{\partial \tau} = \frac{dx_n(R)}{dz} = -f(R_+), \tag{A7}$$

so

$$\frac{\partial x(T)}{\partial \tau} = -\left[f(R_+) + \int_{R_-}^{T} \frac{\partial f}{\partial \tau}\, d\zeta\right]. \tag{A8}$$

Eq. A4 may be rewritten as

$$\frac{\partial x(T)}{\partial \zeta} = -\left[f(R_-) + \int_{R_-}^{T} \frac{\partial f}{\partial \zeta}\, d\zeta\right] \tag{A9}$$

Subtracting Eq. A9 from A8 and using Eq. A3 gives

$$\frac{\partial x(T)}{\partial t} = \frac{v_c}{v_c - 1}(f(R_-) - f(R_+)) - \int_{R_-}^{T} \frac{\partial f}{\partial t}\, d\zeta. \tag{A10}$$

Using Eq. 28 this reduces to

$$\frac{\partial x(T)}{\partial t} = \frac{v_c}{v_c - 1}(f(R_-) - f(R_+)). \tag{A11}$$

Since $y(R_-) > (R_+)$, it follows from Eq. A11 that

$$\frac{\partial x(T)}{\partial t} > 0 \qquad T \text{ in } R_4. \tag{31}$$

For any isocline defined by Eq. 31

$$\left(\frac{dt}{dz}\right)_x = -\frac{\partial x}{\partial z}\Big/\frac{\partial x}{\partial t} \tag{A12}$$

Substitution of $\partial x/\partial z$ from Eq. 2 into A12 and use of Eq. A11 gives

$$\left(\frac{dt(T)}{dz}\right)_x = \frac{1}{v_c}\left[1 + \frac{(v_c - 1)f(T)}{f(R_-) - f(R_+)}\right]. \tag{A13}$$

Since T is to the right of R

$$f(T) > f(R_-), \tag{A14}$$

thus, it follows from Eqs. A13 and A14 that

$$\left(\frac{dt(T)}{dz}\right)_x > 1. \tag{32}$$

b. Construction of Isoconcentration Lines in R_4

Any isoconcentration line in R_4 can be determined by integrating Eq. A13 starting from a point on the concentration characteristic OB corresponding to the prescribed concentration, $\bar{x}$. The z coordinate of the point R which appears in the right hand side of Eq. A13 is

$$z(R) = \left(\frac{v_c}{v_c - 1}\right)(t(T) - z(T)/v_c). \tag{A15}$$

Eq. 13a or 15 may be used to compute $f(R_-)$, $f(R_+)$, and $f(T)$.

A more convenient way of integrating Eq. A13, without using either Eq. 13a or 15 may be obtained by inverting Eq. A13 so that

$$\left(\frac{dz(T)}{dt(T)}\right)_x = \frac{v_c(f(R_-) - f(R_+))}{f(R_-) - f(R_+) + (v_c - 1)f(T)} \tag{A16}$$

and then changing the independent variable from $t(T)$ to $z(R)$. This is done by differentiating Eq. A15 with respect $t(T)$ and using Eq. A16 to obtain

$$\left(\frac{dz(R)}{dt(T)}\right)_x = \frac{v_c f(T)}{f(R_-) - f(R_+) + (v_c - 1)f(T)}. \tag{A17}$$

Dividing Eq. A16 by Eq. A17 gives

$$\frac{dz(T)}{dz(R)} = \frac{f(R_-) - f(R_+)}{f(T)}. \tag{A18}$$

The extended and new steady states exist to the right and left of OA, respectively. Thus, $y(R_-)$ and $y(R_+)$ can be evaluated by solving

$$\frac{dy_e(R)}{dz(R)} = \beta F(y_e) \tag{A19}$$

$$\frac{dy_u(R)}{dz(R)} = \beta F(y_u) \tag{A20}$$

where F is defined by Eq. 11. Combining Eqs. A18 and 6 gives

$$\frac{dy(T)}{dz(R)} = \frac{\beta F(T)\,[f(R_-) - f(R_+)]}{f(T)} \tag{A21}$$

An isoconcentration line corresponding to $\bar{x}$ can be determined by integrating simultaneously Eqs. A18-A21 subject to the following initial conditions at $z(R) = 0$

$$\begin{aligned} y_e(0) &= 1 \qquad y_u(0) = \theta \\ y(T(0)) &= y_i(z_{\bar{x}}) \qquad z(T(0)) = z_{\bar{x}} \end{aligned} \tag{A22a}$$

where $z_{\bar{x}}$ is the value of z for which $x_i(z) = \bar{x}$. The line of zero concentration is determined by setting

$$y(T(0)) = y_{ci} \qquad z(T(0)) = z_{ci}. \tag{A22b}$$

c. A Proof of Eqs. 43, 44, and 48

Set $n = 1$ in Eqs. 23 and 24 and $U = 0$ in Eq. 24. Differentiation of Eq. 24 with respect to ζ gives

$$\frac{\partial^2 y}{\partial\zeta\partial\tau} = \beta\frac{\partial x}{\partial\zeta} f\eta + \beta x\frac{\partial}{\partial\zeta}(f\eta). \tag{A23}$$

Since

$$\frac{\partial}{\partial\zeta}(f\eta) = \frac{d}{dy}(f\eta)\frac{\partial y}{\partial\zeta} \tag{A24}$$

and

$$\frac{\partial}{\partial\tau}(f\eta) = \frac{d}{dy}(f\eta)\frac{\partial y}{\partial\tau} = \beta x f\eta\frac{d}{dy}(f\eta) \tag{A25}$$

then

$$\beta x\frac{\partial}{\partial\zeta}(f\eta) = (f\eta)^{-1}\frac{\partial}{\partial\tau}(f\eta)\frac{\partial y}{\partial\zeta}. \tag{A26}$$

It follows from Eqs. 23 and 24 that

$$\beta\frac{\partial x}{\partial\zeta} = -\frac{\partial y}{\partial\tau}. \tag{A27}$$

Substitution of Eqs. A26 and A27 into Eq. A23 and interchanging the order of differentiation gives

$$\frac{\partial}{\partial\tau}\left(\frac{\partial y}{\partial\zeta}\right) = -f\eta\frac{\partial y}{\partial\tau} + (f\eta)^{-1}\frac{\partial}{\partial\tau}(f\eta)\frac{\partial y}{\partial\zeta}. \tag{A28}$$

Dividing Eq. A28 by $f\eta$ and rearranging gives

$$(f\eta)^{-1}\frac{\partial}{\partial\tau}\left(\frac{\partial y}{\partial\zeta}\right) - (f\eta)^{-2}\frac{\partial}{\partial\tau}(f\eta)\frac{\partial y}{\partial\zeta} + \frac{\partial y}{\partial\tau} = 0. \tag{A29}$$

Therefore,

$$\frac{\partial}{\partial\tau}\left[(f\eta)^{-1}\frac{\partial y}{\partial\zeta} + y\right] = 0. \tag{A30}$$

Integrating Eq. A29 along the y characteristic ST (see Figure 2) yields:

$$\left[(f\eta)^{-1}\frac{\partial y}{\partial\zeta} + y\right]_T = \left[(f\eta)^{-1}\frac{\partial y}{\partial\zeta} + y\right]_S. \tag{A31}$$

Since y at S satisfies the steady-state equations,

$$\left[(f\eta)^{-1}\frac{\partial y}{\partial\zeta} + y\right]_S = \left[(f\eta)^{-1}\frac{dy}{dz} + y\right]_S = [\beta x + y]_S. \tag{A32}$$

It follows from Eqs. 4, 19, A31 and A32 that

$$\frac{\partial y}{\partial\zeta} = f(y)\,\eta(y, \phi_o)\,[1 + \beta - y]. \tag{44}$$

Dividing Eq. 44 by Eq. 23 gives

$$\left(\frac{dy}{dx}\right)_\tau = -\frac{1 + \beta - y}{x}. \tag{A33}$$

Integration of Eq. A33 along the x characteristic RT gives

$$\frac{y(T) - (1 + \beta)}{y(R_-) - (1 + \beta)} = \frac{x(T)}{x(R)}. \tag{48}$$

Using Eq. A3, 24 and 44, we obtain

$$\frac{\partial y(T)}{\partial t} = \frac{v_c}{v_c - 1}[\beta x(T) + y(T) - (1 + \beta)]f\eta. \tag{A34}$$

Replacing $x(T)$ in Eq. A34 by that obtained from Eq. 48 gives

$$\frac{\partial y(T)}{\partial t} = \frac{v_c}{v_c - 1}[\beta x(R) + y(R_-) - (1 + \beta)]\frac{y(T) - (1 + \beta)}{y(R_-) - (1 + \beta)}f\eta. \tag{A35}$$

Thus, the sign of $\partial y/\partial t$ is that of $\beta x(R) + y(R_-) - (1 + \beta)$. From Eq. 19

$$\beta x(R) = \beta + \theta - y_n(R), \tag{A36}$$

so that

$$\beta x(R) + y(R_-) - (1 + \beta) = y(R_-) - y_n(R) - (1 - \theta). \tag{A37}$$

Combining Eqs. A35, A37 and 58 gives

$$\frac{\partial y(T)}{\partial t} > 0. \tag{43}$$

d. Proof of Eq. 60

Writing Eq. 54 for two values of the Thiele modulus satisfying Eq. 61

$$\frac{dy_{-i}(y_n)}{dy_n} = F_i(y_{-i}, y_n) \qquad i = 1, 2 \tag{A38}$$

where

$$F_i(y_{-i}, y_n) = \frac{f(y_{-i})\eta(y_{-i}, \phi_{oi})}{f(y_n)\eta(y_n, \phi_{oi})} \tag{A39}$$

Since η is a monotonic decreasing function of ϕ_o then from Eq. 61

$$0 < F_1(y_{-1}, y_n) < F_2(y_{-2}, y_n) \tag{A40}$$

The initial conditions are

$$y_{-i}(\theta) = 1 \qquad i = 1, 2 \tag{A41}$$

It follows from Eqs. A38, A40 and a theorem about differential inequalities that (Szarski, 1965)

$$y_{-2}(y_n) > y_{-1}(y_n). \tag{A42}$$

Since y_{-i} is a monotonic increasing function of y_n and

$$y_n(z, \phi_{02}) > y_n(z, \phi_{01}) \tag{A43}$$

it follows that

$$y_-(R, \phi_{02}) > y_-(R, \phi_{01}) \qquad \text{Q.E.D.} \tag{60}$$

NOTATION

A = pre-exponential factor
C_A = concentration of species A
c_f = specific heat of fluid
c_s = specific heat of catalyst
D_e = effective diffusivity
E = activation energy
$f(y)$ = dimensionless reaction rate constant
ΔH = enthalpy of reaction
$\hat{k}(T)$ = reaction rate constant $= \rho_s S_g A(1 - \epsilon)/\epsilon \exp(-\gamma/y)$
n = reaction order
R = universal gas constant
R_t = radius of reactor
S_g = catalytic surface area/mass of catalyst particle
S_x = external surface area of catalyst particle
T = temperature
t = dimensionless time
t' = time
U = dimensionless overall heat transfer capacity
U' = overall heat transfer coefficient
u = interstitial velocity
v_c = dimensionless species velocity
V_p = volume of catalyst particle
x = dimensionless concentration
y = dimensionless temperature
y_p = dimensionless limiting transient-peak temperature
z = dimensionless axial position coordinate
z' = axial position coordinate
z_c = dimensionless completion length
z_{cr} = dimensionless critical reactor length
z_r = dimensionless length of the reactor

Greek Letters

β = dimensionless adiabatic temperature rise
γ = dimensionless activation energy
ϵ = void fraction of the bed
ϵ_p = porosity of a catalyst particle
ζ = length along a concentration characteristic
η = effectiveness factor
θ = dimensionless feed temperature, $t > 0$
ρ_f = density of fluid
ρ_s = density of catalyst
τ = length along a temperature characteristic
ϕ_o = Thiele modulus

Subscripts

i = initial steady-state
n = new steady-state
s = arbitrary steady-state
w = wall
o = feed, $t < 0$
$-$ = limit from right side of discontinuity

LITERATURE CITED

Abramowitz, M. and I. A. Stegun, *Handbook of Mathematical Functions*, Dover Publications, Inc., New York, NY (1971).

Aris, R., and N. R. Amundson, *Mathematical Methods in Chemical Engineering*, **2**, Prentice Hall, Englewood Cliffs, NJ (1973).

Auslander, D. M., Y. Takahashi, and M. J. Rabins, *Introducing Systems and Control*, McGraw-Hill, New York, NY (1974).

Boreskov, G. K. and M. G. Slinko, "Modelling of Chemical Reactors," *Pure Appl. Chem.*, **10**, 611 (1965).

Crider, J. E., and A. S. Foss, "Computational Studies of Transients in Packed Tubular Chemical Reactors," *AIChE J.*, **12**, 514 (1966).

Douglas, J. M., and L. C. Eagleton, "Analytic Solutions for Some Adiabatic Reactor Problems," *Ind. Eng. Chem. Fundamentals*, **1**, 116 (1962).

Eigenberger, G., "Influence of the Wall on the Dynamic Behavior of Homogeneous Tubular Reactors with a Highly Exothermic Reaction," *Advances in Chem. Ser.*, **133**, 477 (1974).

Hansen, K. W., and S. B. Jorgensen, "Experimental Investigation of the Dynamics of a Catalytic Fixed-Bed Reactor," *Advances in Chem. Ser.*, **133**, 505 (1974).

Hoiberg, J. A., B. C. Lyche, and A. S. Foss, "Experimental Evaluation of Dynamic Models for a Fixed-Bed Catalytic Reactor," *AIChE J.*, **17**, 1434 (1971).

Luyben, W. L., *Process Modeling, Simulation, and Control for Chemical Engineers*, McGraw-Hill, New York, NY (1973).

McGreavy, C. and H. M. Naim, "Reduced Dynamic Model of a Fixed-Bed Reactor," *Can. J. Chem. Eng.*, **55**, 326 (1977).

Mehta, P. S., "Transient Temperature Excursions in Adiabatic Packed-Bed Reactors—The Pseudohomogeneous Model," Ph.D. dissertation, University of Houston, Houston, Texas (1978).

Sampath, B. S., P. A. Ramachandran, and R. Hughes, "Modelling of Non-Catalytic Gas-Solid Reactions-II, Transient Simulation of a Packed-Bed Reactor," *Chem. Eng. Sci.*, **30**, 135 (1975).

Sharma, C. S. and R. Hughes, "The Behavior of an Adiabatic Fixed-Bed Reactor for the Oxidation of Carbon Monoxide Part 2: Effect of Perturbations," *Chem. Eng. Sci.*, **34**, 625 (1979).

Szarski, J., *Differential Inequalities*, Hafner, New York, NY (1975).

Van Doesburg, H., and W. A. DeJong, "Transient Behavior of an Adiabatic Fixed-Bed Methanator: I. Experiments with Binary Feeds of CO or CO_2 in Hydrogen," *Chem. Eng. Sci.*, **31**, 45 (1976a).

Van Doesburg, H., and W. A. DeJong, "Transient Behavior of an Adiabatic Fixed-Bed Methanator: II, Methanation of Mixtures of Carbon Monoxide and Carbon Dioxide," *Chem. Eng. Sci.*, **31**, 53 (1976b).

Manuscript received May 7, 1980, revision received July 10, and accepted July 16, 1980.